JOURNAL OF GEOPHYSICAL RESEARCH, VOL. 113, C09035, doi:10.1029/2008JC004796, 2008

Estimation of the sea level trend south of Japan by combining satellite altimeter data with in situ hydrographic data

Hiroshi Uchida[1] and Shiro Imawaki[2,3]

Received 2 March 2008; revised 19 June 2008; accepted 16 July 2008; published 30 September 2008.

[1] The sea level trend from1992 to 2006 was estimated by combining satellite altimeter data with in situ hydrographic data along the TOPEX/POSEIDON and Jason-1 subsatellite track south of Japan. The sea level trend estimates from the altimeter data were consistent with those from the coastal tide gauge data. The mean sea level trend along the hydrographic observation line was 4.2 ± 0.8 mm a^{-1}. By assuming that the sea level trend due to large-scale deformation of ocean basins from glacial isostatic adjustment is −0.3 mm a^{-1}, the sea level trend by the ocean mass change was estimated to be 1.3 ± 0.4 mm a^{-1}, and the steric height trend was estimated to be 3.2 ± 0.9 mm a^{-1} (2.8 ± 0.9 mm a^{-1} between 0 and 1800 dbar plus 0.4 ± 0.2 mm a^{-1} between 1800 and 4500 dbar). Steric height estimated from the altimeter data agreed well with that estimated from the conductivity-temperature-depth profiler and expendable bathythermograph data. However, steric height estimated from the Argo float data over year 2004−2006 was significantly biased of about −10 mm on average with respect to that estimated from the altimeter data. A systematic pressure error of about −2 dbar in the Argo float profiles could account for this negative bias in steric height.

Citation: Uchida, H., and S. Imawaki (2008), Estimation of the sea level trend south of Japan by combining satellite altimeter data with in situ hydrographic data, *J. Geophys. Res.*, *113*, C09035, doi:10.1029/2008JC004796.

1. Introduction

[2] Global mean sea level change can be a sign of climate change such as global warming. Recently, it has become possible to evaluate the ocean mass change and steric height components of the global mean sea level trend by combining sea level data from satellite altimeters with time-variable gravity data from the Gravity Recovery and Climate Experiment (GRACE) space mission [*Lombard et al.*, 2007]. However, the steric height trend estimated from the satellite data (positive trend) disagreed with that from the in situ hydrographic data (negative trend) during the period from mid-2003 to 2005 [*Lombard et al.*, 2007]. The negative steric height trend from the in situ data was associated with rapid cooling of the upper ocean [*Lyman et al.*, 2006], but the apparent rapid cooling was caused in part by a systematic bias in a subset of Argo float profiles [*Lyman et al.*, 2006]. *Lyman et al.* [2006] also suggested that a systematic bias present in expendable bathythermograph (XBT) data [*Gouretski and Koltermann*, 2007] also contributed to the apparent rapid cooling. Meanwhile, *Uchida et al.* [2008] suggested that at present most Argo float pressure data may have a systematic negative bias, which may also contribute to the apparent rapid cooling.

[1]Institute of Observational Research for Global Change, Japan Agency for Marine-Earth Science and Technology, Yokosuka, Japan.

[2]Research Institute for Applied Mechanics, Kyushu University, Kasuga, Japan.

[3]Now at Japan Agency for Marine-Earth Science and Technology, Yokosuka, Japan.

0148-0227/08/2008JC004796$09.00

[3] Since 1992, repeated hydrographic observations were carried out along the TOPEX/POSEIDON subsatellite track south of Japan (Figure 1) by a group called ASUKA [*Imawaki et al.*, 2001] and, especially, the Japan Meteorological Agency (JMA). Conductivity-temperature-depth profiler (CTD), XBT, and expendable CTD (XCTD) data were accumulated during more than 140 cruises along the observation line (Figure 2). Therefore, altimeter data along the observation line (ASUKA line) can be compared precisely with in situ hydrographic data without applying smoothing techniques or averaging the data over a wide area or over a long term. Moreover, the ASUKA line is suitable for validation of the altimeter data by using coastal tide gauge data, since a tide gauge station is located near the ASUKA line (Figure 1).

[4] The current study presents estimates of the sea level trend along the ASUKA line between September 1992 and December 2006. The sea level trend estimated from the altimeter data was compared with that estimated from the tide gauge data. By combining the altimeter data with the ship-based CTD data, components of the sea level trend due to ocean mass and steric height changes were also estimated. Steric heights estimated from the altimeter data were then compared with those estimated from the ship-based hydrographic data and the Argo profiling float data along the ASUKA line to investigate how well they corresponded.

2. Data and Data Processing

[5] The satellite altimeter data used were TOPEX/POSEIDON and Jason-1 along-track sea level anomalies

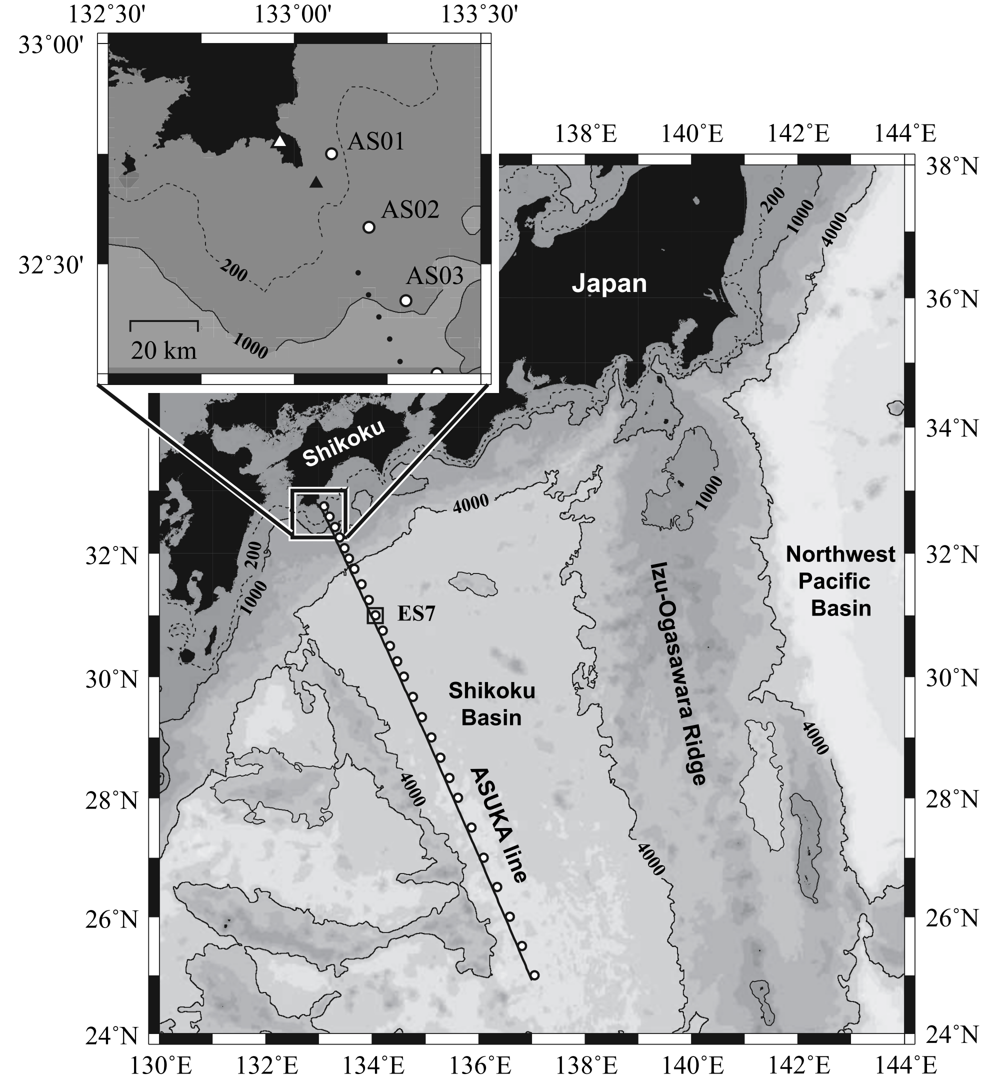

Figure 1. Standard locations of hydrographic stations (open circles) along the ASUKA observation line southeast of Shikoku, Japan. The square indicates the PIES mooring station (ES7). The observation line was purposely located along the track of the TOPEX/POSEIDON satellite altimeter (solid line and small dots in the inset). The open triangle indicates the location of the tide gauge station. The solid triangle indicates the northernmost point of the satellite track. Selected bottom topography contours (m) are also shown.

produced by SSALTO/DUACS and distributed by AVISO, France. The delayed time products (up-to-date data sets) were produced every 10 days for a period of 14 years, from September 1992 to December 2006. Hourly sea level data obtained at a coastal tide gauge station (Tosashimizu) (Figure 1) were also used to validate the altimeter data and to fill in the gap in the altimeter data near the coast. An inverted barometer correction was applied to the tide gauge sea level data by using hourly atmospheric pressure data obtained at a nearby meteorological station (Shimizu). Tidal period fluctuations were removed from the tide gauge sea level data by using a 48-h tide killer filter [*Hanawa and Mitsudera*, 1985], and then sea level anomalies from the temporal mean of the period from 1993 to 1999 were calculated by using the same definition as was used for the altimeter data. The sea level anomalies were interpolated into the altimeter data time series, and were used to supplement the altimeter data at the northern end of the satellite track (solid triangle in Figure 1). The sea level anomaly profiles along the ASUKA line were smoothed and interpolated by using a state space method for estimation of smooth trends (second-order state space trend model) [*Kitagawa and Gersch*, 1996].

[6] Gridded sea level anomaly data produced by SSALTO/DUACS were also used to estimate sea level trend over the Shikoku Basin (Figure 1). The data were delayed time multimission (TOPEX/POSEIDON or Jason-1 plus ERS-1/2 or Envisat) products (up-to-date data sets) produced every 7 days with a resolution of quarter degrees in both latitude and longitude.

[7] Ship-based hydrographic data along the ASUKA line were collected by four types of instrument: CTD, XCTD, XBT, and digital bathythermograph (DBT). The CTD data were reported at 1- or 2-dbar intervals. The XCTD, XBT,

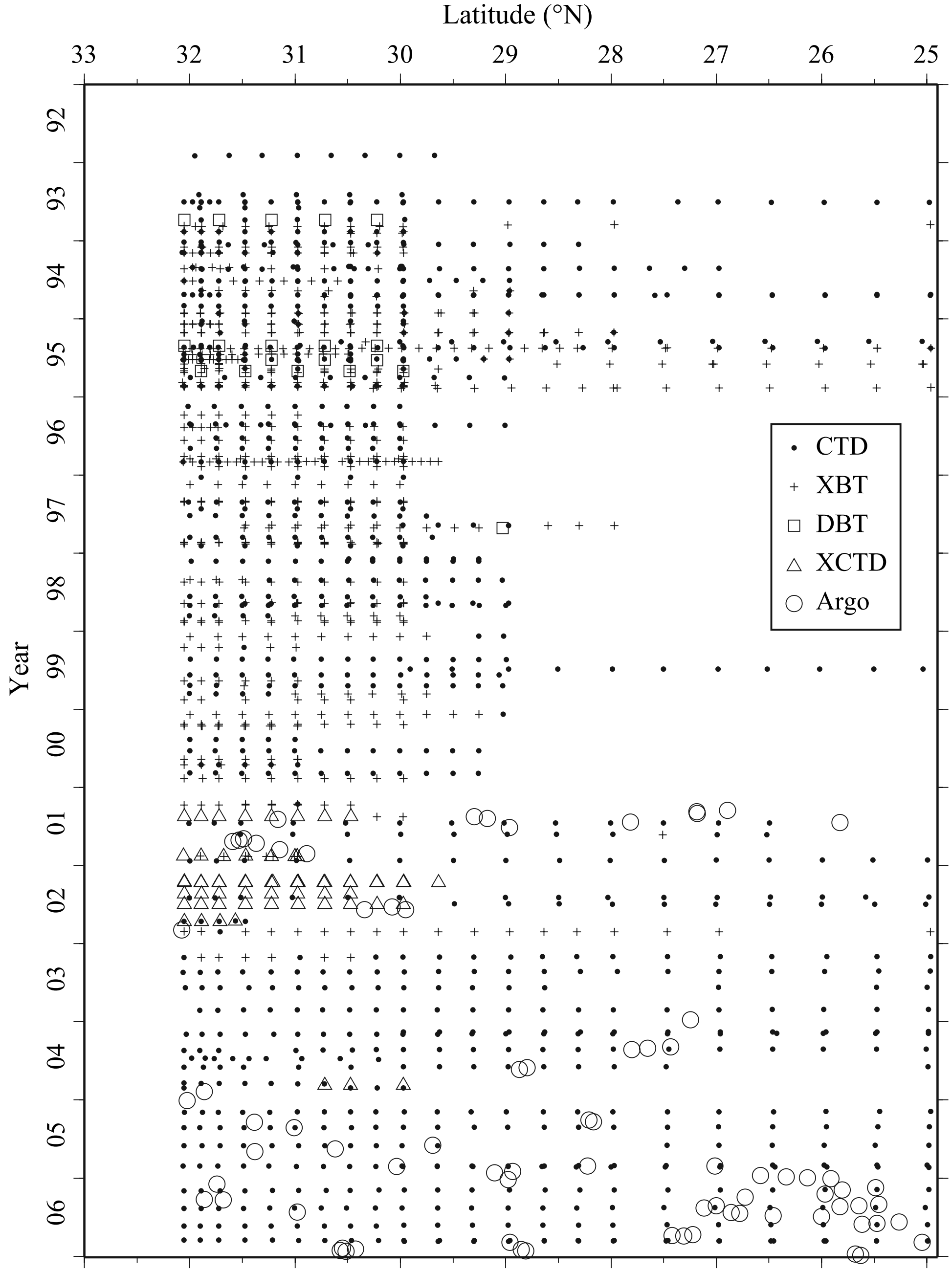

Figure 2. Hydrographic data distribution along the ASUKA line.

and DBT data were carefully processed to 1-dbar intervals as follows.

[8] Raw data from the XBT (20 samples s^{-1}) and the fall rate equation of *Hanawa et al.* [1995] for the T-7 and T-6 probes and that of *Kizu et al.* [2005] for the T-5 probe were used to infer depth. Pressure (p in dbar) was estimated from the inferred depth (z in m) by using the simplified equation, $p = z/0.993$, after *Hanawa et al.* [1995]. The first eight scans (about 3 dbar) of the XBT data were deleted, and then the data were low-pass-filtered using a median filter with a window of five scans (about 1.3 m). Then, the data were sampled at 1-dbar intervals. To calculate steric height from the XBT data, it was necessary to determine salinity profiles, because only temperature profiles were obtained from the XBT measurements. Salinity profiles for the XBT measurements were estimated by using mean temperature–salinity relations (see Appendix A for details). About half (52%) of the XBT profiles were obtained by using Sparton T-7 probe (Sparton of Canada Ltd., Ontario, Canada) and the rest of the profiles were obtained by using TSK T-7 (41%), T-6 (4%), and T-5 (3%) probes (Tsurumi-Seiki Co. Ltd., Kanagawa, Japan).

[9] Pressure was estimated from the DBT data, which were reported at 1-m intervals, by using the same method as for the XBT data. Then the DBT data were sampled at 1-dbar intervals. Salinity profiles were estimated by using the same method as for the XBT data, because only temperature profiles were obtained from the DBT measurements.

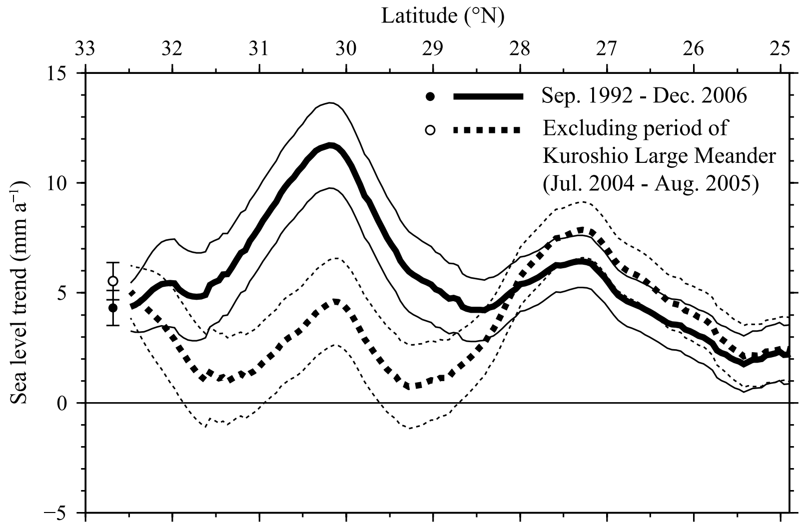

Figure 3. Horizontal distribution of the sea level trend between September 1992 and December 2006 calculated from altimeter (thick line) data and tide gauge (circles) data. The data indicated by the thick dashed line and open circle were calculated by excluding data collected during the Kuroshio large meander from July 2004 to August 2005. The vertical bars (tide gauge data) and thin solid and dashed lines (altimeter data) indicate the estimated errors.

[10] Raw temperature and conductivity data from the first nine scans of the XCTD data were deleted, and then the remaining data were low-pass-filtered using a boxcar filter with a window of 15 scans (about 2 m). The conductivity data were advanced by two scans (about 0.3 m) relative to the temperature data to correct for a mismatch in the response times of the sensors. Pressure was estimated from depth and location (latitude) by calculating backward using a pressure-to-depth conversion equation [*Saunders and Fofonoff*, 1976], and salinity was calculated from the pressure, temperature, and conductivity data by using the reference conductivity of 4.2896 S m^{-1} at a salinity of 35, a temperature of 15°C, and a pressure of 0 dbar. Then, the data were sampled at 1-dbar intervals. Biases of the salinity profiles were estimated by using the tight relationships between temperature and salinity at temperatures of 14.1 and 2.5°C (Appendix A), and the estimated biases were then subtracted from the salinity profiles. A salinity of 34.542 for a temperature of 14.1°C and of 34.535 for a temperature of 2.5°C were used regardless of time and location.

[11] Argo profiling float data were provided by IFREMER Global Data Center in June 2007 and were used when their locations were within 0.2° longitude from the ASUKA line (Figure 2). About one third of the data obtained from 23 floats were quality controlled delayed-mode data and the rest of the data were real-time data. Temperature and salinity data were vertically interpolated at 2-dbar intervals by a piecewise cubic Hermite spline interpolation [*de Boor*, 2001]. Biases of the salinity profiles were corrected by using the same method as for the XCTD data, when the magnitude of the estimated bias was greater than 0.03.

[12] To investigate short-term fluctuations of nonsteric height, pressure data obtained from pressure sensor-equipped inverted echo sounders (PIES) (Smart IES model 1050; Marine Systems Technology, North Falmouth, Massachusetts) at sea bottom (about 4400 m) at 31°N on the ASUKA line (square in Figure 1) were used. Details of the PIES observations were described by *Kakinoki et al.* [2008]. Since the pressure sensors (Digiquartz model 9010K-101; Paroscientific Inc., Redmond, Washington) were drifted in time, the time drifts in the pressure data were estimated by fitting exponential-linear curves [*Watts and Kontoyiannis*, 1990] and were removed from the data. After major eight tidal constituents (K1, O1, P1, Q1, M2, S2, N2, and K2) were removed by harmonic analysis, the pressure data were low-pass-filtered by using the Butterworth filter with a 50-h cutoff period and were resampled at 6-h intervals. The pressure anomalies p' from the temporal mean of the mooring observation period were calculated, and then nonsteric height anomalies d' were calculated as follows: $d' = p' (g\rho_b)^{-1}$, where g is the gravitational acceleration, and ρ_b is the density near the bottom.

3. Estimation of the Sea Level Trend

3.1. Sea Level Trend From Altimeter Data

[13] The sea level trend between September 1992 and December 2006 along the ASUKA line was calculated from the altimeter and tide gauge data by using the least squares method to calculate the best fit linear trend (Figure 3). The sea level trend estimates from the altimeter data were consistent with those from the coastal tide gauge data near the coast. The size of the sea level trend varied widely by location (from 2 to 12 mm a^{-1}), and the mean sea level trend (5.7 ± 0.8 mm a^{-1}) north of 25°N was much larger than the global mean sea level trend (3.16 ± 0.03 mm a^{-1}) between 1993 and 2006 calculated from altimeter data (a time series of global mean sea level was created by AVISO and is available online at http://www.aviso.oceanobs.com/).

[14] The relatively large sea level trend at around 30°N (Figure 3) may be associated with a Kuroshio large meander

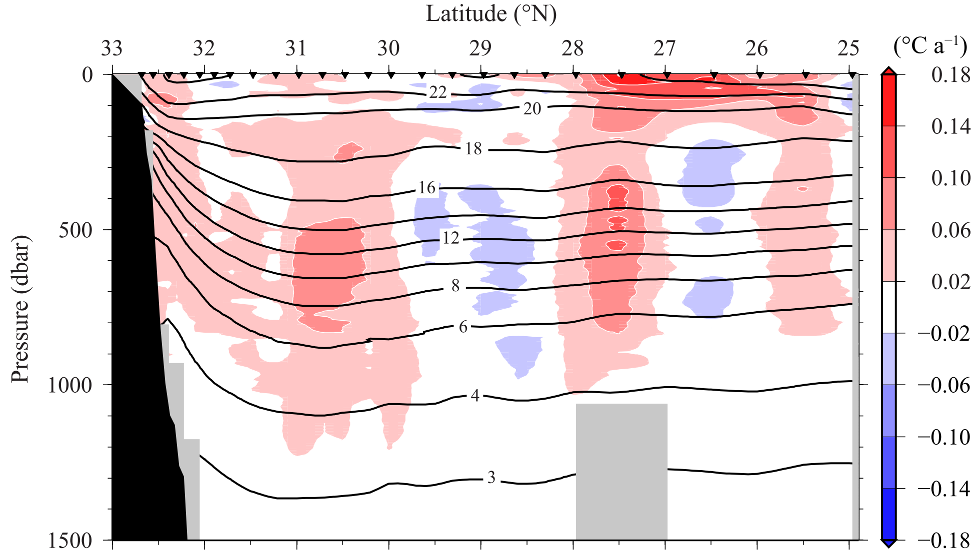

Figure 4. Vertical section of the temporal mean potential temperature (°C) (contours) and the temperature trend (color) estimated from the ASUKA hydrographic data. The mean potential temperature was calculated for each 2-year box at the standard hydrographic locations (inverted triangles), and then the temperature trend was estimated from the mean temperature at each depth, when the means were calculated from more than two data points, using the least squares method. The temporal mean potential temperature was estimated for the middle of the data period (1 January 2000) from the temperature trend. For depths shallower than 200 dbar, the seasonal temperature and salinity signals were subtracted in advance by using the best fitting curve of the sum of annual and semiannual sine curves for each depth, regardless of year and location.

that occurred in 2004/2005, near the end of the data collection period, and strengthened the local stationary anticyclonic warm eddy off Shikoku. The temperature trend estimated from the ASUKA hydrographic data showed a warming in the thermocline at around 30–31°N (Figure 4), suggesting a deepening of the thermocline corresponding to the strengthening of the anticyclonic warm eddy. In fact, the sea level trend at around 30°N was reduced when the data collected during the Kuroshio large meander (July 2004 to August 2005) were excluded (Figure 3). To understand the structure of the variability, time series of spatially averaged sea level anomalies were examined (Figure 5). The sea level anomaly averaged over north of 28°N along the ASUKA line compared well with the sea level anomaly averaged over the Shikoku Basin in the 1990s, but did not in the 2000s. It fluctuated largely and the discrepancy exceeded

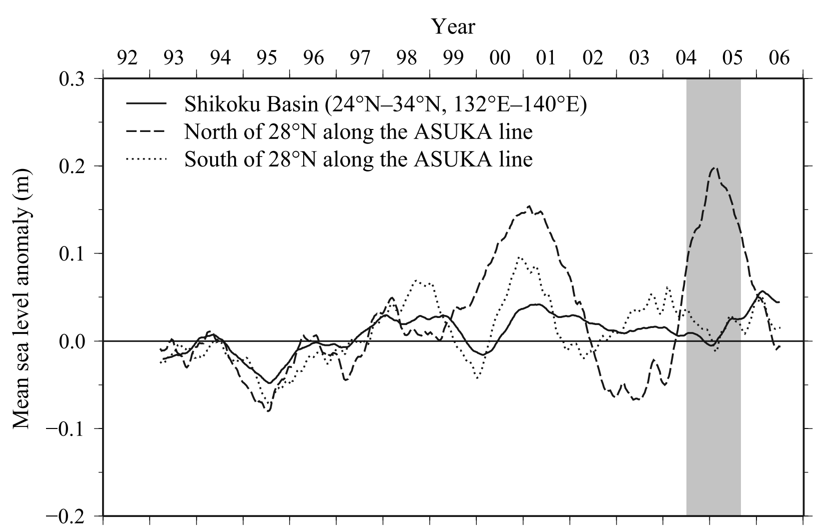

Figure 5. Time series of spatially averaged sea level anomalies. The sea level anomalies were low-pass-filtered by the running mean with a window of 1 year. The Kuroshio large meander period is shown by the shading.

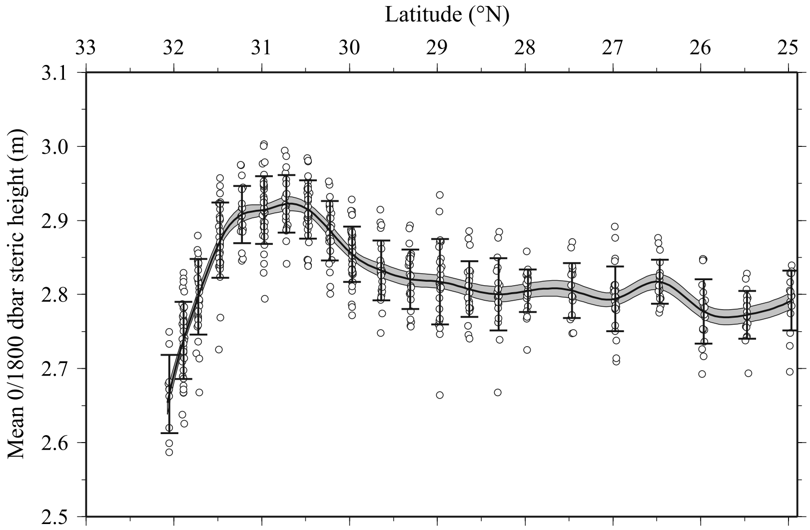

Figure 6. Horizontal distribution of mean 0/1800 dbar steric heights. Circles are individual estimates obtained by combining altimeter data with CTD data (see text for details). The mean 0/1800 dbar steric heights (thick line) with standard errors (shade) estimated at standard hydrographic stations were interpolated horizontally by piecewise cubic Hermite spline interpolation. The mean of the errors was 0.009 m. Vertical bars show standard deviations at the standard hydrographic stations; the mean of the standard deviations was 0.042 m.

0.1 m, especially in the Kuroshio large meander period (0.2 m). On the other hand, the sea level anomaly averaged over south of 28°N along the ASUKA line agreed well with the sea level anomaly averaged over the Shikoku Basin and was not influenced by the Kuroshio large meander (Figure 5). Therefore the mean sea level trend (4.2 ± 0.8 mm a^{-1}) south of 28°N was considered to be a robust estimate of the mean sea level trend of the ASUKA line. The estimated trend agreed with the mean sea level trend (3.7 ± 0.3 mm a^{-1}) over the Shikoku Basin within the error and became close to the global mean (3.16 ± 0.03 mm a^{-1}).

3.2. Steric and Nonsteric Height Trends

[15] The sea level trend estimated from the altimeter data consists of both steric and nonsteric height trends. Since in situ hydrographic data provide steric height information, steric and nonsteric height trends along the ASUKA line can be estimated by combining the altimeter data with the hydrographic data. In order to accurately calculate steric height, full-depth temperature and salinity profiles are needed, but we considered the steric height between 0 and 1800 dbar (hereafter, steric height calculated between *A* and *B* dbar is denoted the *A*/*B* dbar steric height) adequate to estimate the nonsteric height trend.

[16] The nonsteric height trend was estimated by using a similar method to that of *Uchida et al.* [1998], with modification. At location x and time t, the 0/1800 dbar steric height $h(x, t)$ is written as follows:

$$h(x,t) = \overline{h(x)} + h'(x,t) \tag{1}$$

where $\overline{h(x)}$ is the temporal mean steric height and $h'(x, t)$ is the steric height anomaly. The 0/1800 dbar steric height $h(x, t)$ was calculated repeatedly from the CTD data. Meanwhile, the altimeter-derived sea level anomaly $z'(x, t)$ was approximated as $z'(x, t) = h'(x, t) + d'(t)$, ignoring the nonsteric height fluctuation except for the nonsteric height linear trend $d'(t)$, regardless of location. If the CTD data is randomly distributed in space and time against the nonsteric height fluctuation, the nonsteric height trend can be estimated accurately. The validity of this assumption is discussed in section 4. Therefore equation (1) can be modified as follows:

$$h(x,t) = \overline{h(x)} + z'(x,t) - d'(t). \tag{2}$$

The unknown temporal mean steric height $\overline{h(x)}$ and the nonsteric height trend $d'(t)$ were estimated from equation (2) by using the least squares method. The model parameters ($\overline{h(x)}$ and a coefficient a of $d'(t)$) were obtained by minimizing the quantity

$$\chi^2 \equiv \frac{1}{s^2} \sum_{i=1}^{n} \left\{ y_i(x,t) - \left[\overline{h(x)} - at \right] \right\}^2 \tag{3}$$

where $y_i(x, t) = h_i(x, t) - z_i'(x, t)$, s is an uncertainty associated with a set of measurements, and n is a number of measurements. The altimeter data obtained at 10-day intervals were interpolated into the hydrographic data time series and used with the adequately large number (519) of hydrographic data collected at standard hydrographic stations (22 stations). The temporal mean denotes the 7-year mean (1993 to 1999), which was the definition of anomaly used for the altimeter data. Reference of time t was defined as middle of the 7-year. The horizontal distribution of the temporal mean 0/1800 dbar steric height is shown in Figure 6. The nonsteric height trend was thus estimated to be 1.4 ± 0.4 mm a^{-1}. The steric height trend below 1800

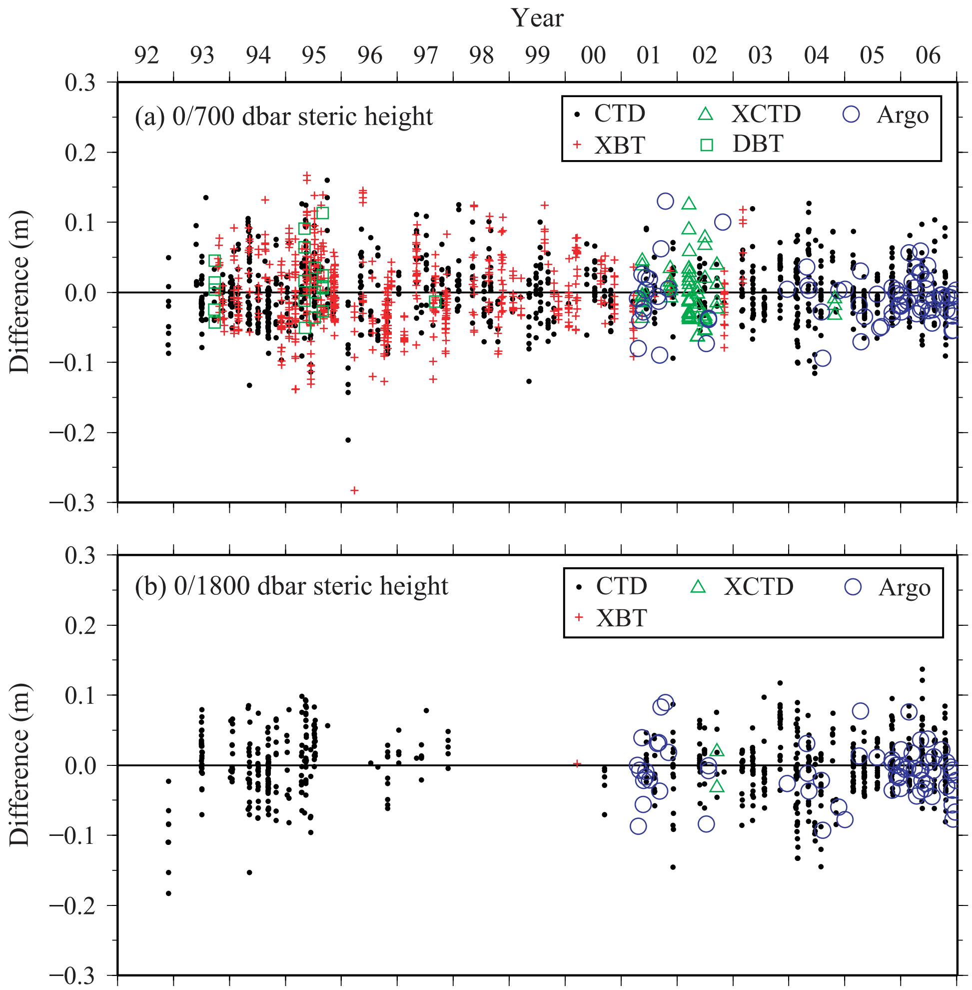

Figure 7. Differences between steric height calculated from hydrographic data and that estimated from altimeter data for (a) 0/700 dbar and (b) 0/1800 dbar steric heights.

dbar may contaminate the nonsteric height trend estimate; this problem is discussed in section 4.

[17] The 0/1800 dbar steric height trend was estimated to be 2.8 ± 0.9 mm a^{-1} by subtracting the nonsteric height trend (1.4 ± 0.4 mm a^{-1}) from the mean sea level trend (4.2 ± 0.8 mm a^{-1}) south of 28°N along the ASUKA line.

3.3. Comparison of Steric Heights Estimated From Altimeter and Hydrographic Data

[18] The time series of the 0/1800 dbar steric height was estimated from the altimeter sea level anomaly data by using equation (2). To compare the altimeter data with the XBT, XCTD, DBT, and CTD data obtained by shallow casts, 0/700 dbar steric heights were also estimated from the altimeter data by using the relationship between the 200/1800 dbar steric height and the 200/700 dbar steric height (sea Appendix B for details). The 0/700 and 0/1800 dbar steric heights from the altimeter data obtained at 10-day intervals were interpolated into the hydrographic data time series and compared with the hydrographic data (Figure 7).

[19] First, mean differences between the CTD and altimeter data collected by the TOPEX side A, TOPEX side B, and Jason-1 altimeter sensors were examined (Table 1). Data from the POSEIDON altimeter (9% of TOPEX/POSEIDON observations) were not distinguished from those from the TOPEX altimeter. No significant difference was found between the CTD and altimeter data obtained by each altimeter sensor. These results suggest that systematic biases between the altimeter sensors were well corrected and that the 0/700 dbar steric heights were thus well estimated from the altimeter data. Next, mean differences between the altimeter data and the hydrographic data by instrument type were examined (Table 2). As with the CTD data, no significant difference was found between the altimeter data

Table 1. Mean Steric Height Differences Between Altimeter and CTD Data[a]

	0/700 dbar Steric Height		0/1800 dbar Steric Height	
Altimeter	Mean ± SE (mm)	*n*	Mean ± SE (mm)	*n*
TOPEX-A	−1.6 ± 2.2	471	1.4 ± 3.0	238
TOPEX-B	−1.4 ± 2.9	154	−2.9 ± 4.7	69
Jason-1	0.0 ± 2.1	369	−1.0 ± 2.3	359

[a]The mean was calculated for each altimeter sensor. The TOPEX side A altimeter data were collected from September 1992 to January 1999, the TOPEX side B data were from February 1999 to July 2002, and the Jason-1 data were from August 2002 to December 2006. The number of data points is also shown.

Table 2. Mean Steric Height Differences Between the Altimeter and Hydrographic Data[a]

Instrument	0/700 dbar Steric Height Mean ± SE (mm)	*n*	0/1800 dbar Steric Height Mean ± SE (mm)	*n*
	Whole Period			
CTD	−1.0 ± 1.4	994	−0.3 ± 1.7	666
XBT	0.3 ± 2.0	653	NA	NA
DBT	11.2 ± 10.1	19	NA	NA
XCTD	−2.6 ± 4.7	62	NA	NA
Argo	−8.7 ± 4.3	77	−10.1 ± 4.6	68
	2004–2006			
CTD	−1.0 ± 2.4	287	−2.8 ± 2.7	279
Argo	−10.4 ± 3.8	58	−12.6 ± 4.9	50

[a]The mean was calculated for each hydrographic instrument type. The number of data points is also shown. NA, not available.

and the XBT or XCTD data. Although the mean difference in the DBT data was quite large, the error of the mean value was also large owing to the small number of data points. Unlike the ASUKA hydrographic data results, a significant negative bias was found in the Argo float data relative to the altimeter data.

[20] Differences between the altimeter and Argo float data were examined by pressure sensor type (Table 3). The standard deviation for the result of Druck pressure sensors (Druck, Ltd., Leicester, UK) was small compared to the result of a Paine pressure sensor (Paine Electronics, LLC, East Wenatchee, Washington) or the result of Ametek pressure sensors (Ametek Inc., Paoli, Pennsylvania). However, the mean difference for the result of Druck pressure sensors showed significant negative bias. After 2004, the Argo floats, except for one with an Ametek pressure sensor, were equipped with Druck pressure sensors, and as a result, the mean differences between the altimeter and Argo float data for the period from 2004 to 2006 showed significant negative bias (about −10 mm), although no significant difference was found between the altimeter and CTD data for the same period (Table 2).

[21] The Argo float data were directory compared with the CTD data when the distances of their locations were within 0.1° latitude along the ASUKA line and the time lags of their observations were within 3 days. Four temperature profiles obtained from 4 Argo floats with Druck pressure sensors were compared with 5 CTD temperature profiles (Figure 8). Temperature data derived from the Argo floats were lower than that from the CTD on average in the thermocline (about −0.04°C around 500 dbar), although the estimated errors were quite large owing to the small number of comparisons. As a result, the 0/1800 dbar steric height calculated from the Argo float data was lower than that from the CTD data on average (−7.6 mm). The steric height estimated from the Argo float data had systematic negative bias with respect to the steric height estimated from not only the altimeter data but also the CTD data.

4. Discussion

[22] In section 3, the temporal mean steric height and the nonsteric height trend were estimated by using equation (2), ignoring the nonsteric height fluctuation except for the linear trend. The validity of this assumption is discussed. Discrepancies (standard deviation, 43 mm) between the estimated temporal mean steric height and the individual estimates obtained by combining altimeter data with CTD data (Figure 6) were caused mainly by three factors: nonsteric height fluctuations, steric height fluctuations deeper than 1800 dbar, and observational errors. The short-term fluctuation of nonsteric height was estimated from the bottom pressure time series at 31°N on the ASUKA line (Figure 9). The dominant variability was at a period about 4 months. The short-term fluctuation (standard deviation, 31 mm) represented 52% of the discrepancies. In fact, it agreed with the difference between the 0/1800 dbar steric height estimated from the altimeter and CTD data (circles in Figure 9). The 1800/4500 dbar steric height fluctuation (standard deviation, 15 mm) was estimated from the 221 CTD profiles along the ASUKA line. By assuming that the overall error of the altimeter data is 20 mm, the residual discrepancy is estimated to be 16 mm. The rest of error sources are considered to be difference of sampling scheme in time between the altimeter and CTD data, and the interannual fluctuation of nonsteric height. Most of the residual discrepancy is likely to be the former, because the error due to difference of sampling scheme in time, estimated by using the daily sea level data obtained from the tide gauge, was fairly large (standard deviation, 43 mm).

[23] The annual variation is the most energetic component in the wind stress driving the large-scale ocean circulation. However, the barotropic response of the midlatitude North Pacific Ocean induced by the annual variation in the wind stress east of the Izu-Ogasawara Ridge is prohibited from propagating westward by the Izu-Ogasawara Ridge, and is converted into a baroclinic signal there [*Isobe and Imawaki*, 2002; *Isobe et al.*, 2004]. The baroclinic activity on the ridge occurs for timescales of the wind variation up to several years, and, for the timescale much longer than the time taken for the long baroclinic Rossby wave to cross the ocean, isostasy is accomplished even east of the ridge [*Isobe and Imawaki*, 2002]. Therefore, the barotropic response on the ASUKA line mainly induced by the local wind stress over the Shikoku Basin and must be small compared to the barotropic response east of the Izu-Ogasawara Ridge. In fact, the short-term fluctuation of nonsteric height on the ASUKA line (standard deviation, 31 mm) was small compared to that estimated from 1-year time series of PIES data in the Kuroshio Extension region (near 143°E, 35°N) east of the Izu-Ogasawara Ridge (root-mean-square variability, 41 mm) [*Teague et al.*, 1995].

[24] The nonsteric sea level trend (1.4 ± 0.4 mm a^{-1}) estimated in section 3 includes a small component due to large-scale deformation of ocean basins from glacial iso-

Table 3. Mean 0/1800 dbar Steric Height Differences Between the Altimeter and the Argo Float Data[a]

Pressure Sensor	Mean ± SE (mm)	Number of Floats	Number of Data	SD (mm)
Paine	17.5 ± 17.5	1	6	42.9
Ametek	−18.4 ± 9.9	5	20	44.4
Druck	−10.1 ± 5.1	13	42	33.3

[a]The mean was calculated for each pressure sensor type. The number of floats, the number of data points, and the standard deviations are also shown.

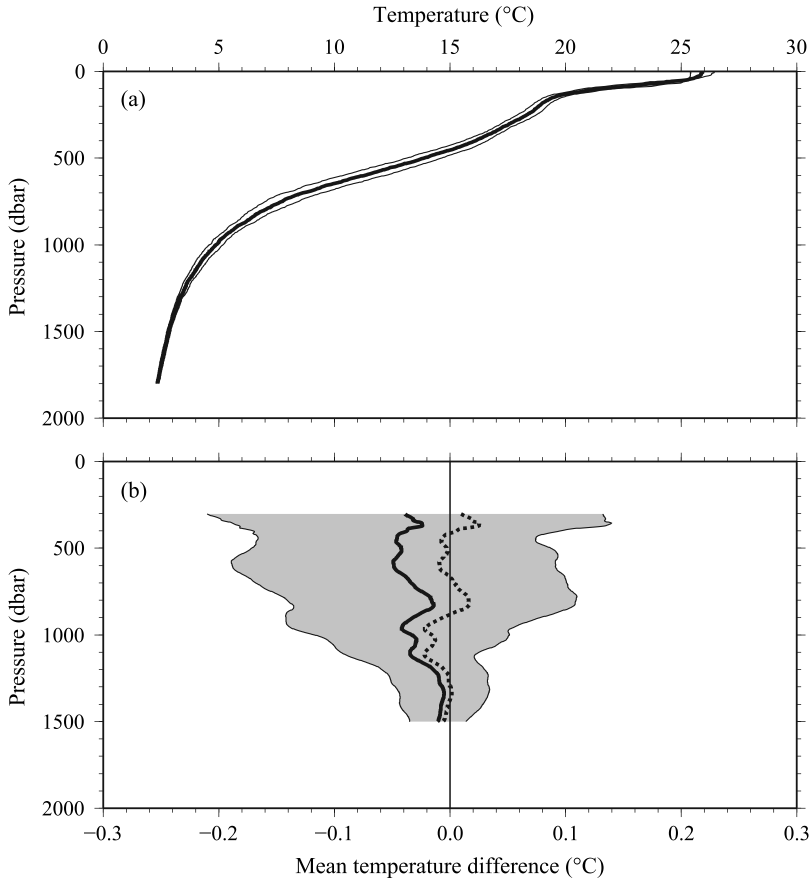

Figure 8. Comparison between the Argo and CTD temperature profiles. (a) Mean temperature profile (thick line) with standard errors (thin lines) of the CTD profiles and (b) mean profile of temperature difference (thick line) with standard errors (shade) between the Argo and CTD data. Four temperature profiles obtained from four Argo floats with Druck pressure sensors were compared with five CTD temperature profiles. The mean profile of temperature difference was low-pass-filtered by the running mean with a window of 600 dbar. When the Argo float data are corrected assuming a systematic pressure error of −2 dbar, the temperature biases seen in the Argo float data almost disappear (dotted line).

static adjustment (GIA). When glaciers and ice sheets are decreasing in size, GIA causes an increase in the volume of the ocean basins, which trends to reduce the global mean sea level. *Lombard et al.* [2007] applied a linear correction (−0.3 mm a^{-1}) to the global mean sea level time series to account for GIA. Moreover, the steric sea level trend deeper than 1800 dbar, which was not taken into account in section 3, contaminates the nonsteric sea level trend estimate. By using the 221 CTD profiles along the ASUKA line, the 1800/4500 dbar steric height trend was estimated to be 0.4 ± 0.2 mm a^{-1}, without taking into account inhomogeneous spatial and temporal distributions of the data. As a result, the steric height trend in the deep layer may mostly compensate for the component from GIA, and the sea level trend by the ocean mass change was estimated to be 1.3 ± 0.4 mm a^{-1}, without taking into account the error in the component from GIA. The estimated sea level trend by the ocean mass change agrees well with previous estimates: 1.2 ± 0.4 mm a^{-1} between 1993 and 2003, based on changes in glaciers, ice caps, the Greenland ice sheet, and the Antarctic ice sheet [*Lemke et al.*, 2007], 1.2 ± 0.5 mm a^{-1} between 2002 and 2006, based on globally averaged GRACE data [*Lombard et al.*, 2007], and 1.4 mm a^{-1} based on freshening of the ocean [*Munk*, 2003]. Meanwhile, the full-depth steric height trend was estimated to be 3.2 ± 0.9 mm a^{-1}, which is 2.8 ± 0.9 mm a^{-1} for 0/1800 dbar plus 0.4 ± 0.2 mm a^{-1} for 1800/4500 dbar.

[25] Instrumental bias was examined in section 3. Steric height estimated from the altimeter data on average agreed with that estimated from the CTD data and the carefully processed XBT data. The negative bias (of about −10 mm) in the steric height found in the Argo float data has rather serious implications for climate research. The magnitude of the bias is comparable to the observed discrepancy in steric height between satellite data and in situ hydrographic data [*Lombard et al.*, 2007]. A systematic pressure error of −2 dbar in the Argo float profiles used would cause an artificial 0/1800 dbar steric height bias of −10 mm. Also, when the Argo float data are corrected assuming a systematic pressure error of −2 dbar, the temperature biases seen in the Argo float data almost disappear (Figure 8). Such a systematic pressure error may exist in the Argo float data [*Uchida et al.*, 2008], and characteristics of the vertical distribution of the initial bias and the time drift of the Argo

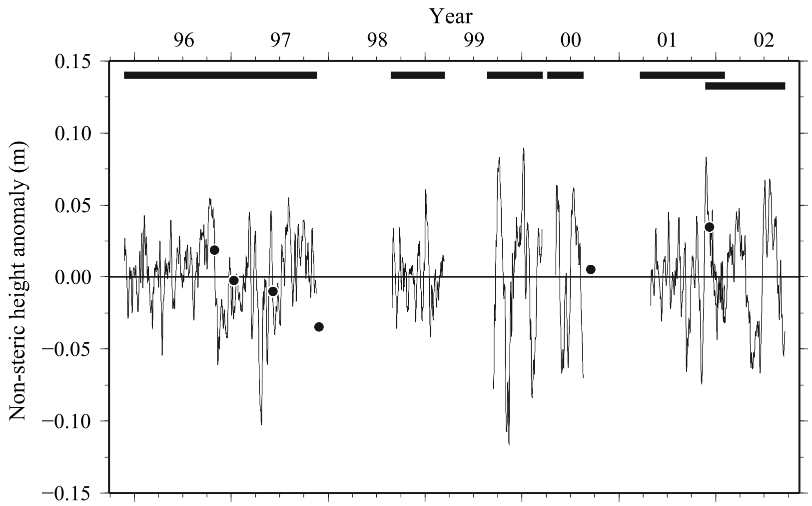

Figure 9. Time series of nonsteric height anomalies calculated from the pressure time series at sea bottom (about 4400 m) at 31°N on the ASUKA line. Nonsteric height anomalies from the temporal mean of the mooring observation period (horizontal bars) were shown. The nonsteric height anomalies were low-pass-filtered by the running mean with a window of 3 days. Circles indicate differences between the 0/1800 dbar steric height estimated from the altimeter and CTD data at that location, and the mean discrepancy between the differences and the nonsteric height anomalies was 8.9 mm (standard deviation, 8.4 mm) for the four comparisons.

pressure sensors and their implications for climate research should be investigated.

Appendix A: Estimation of Salinity Profiles From XBT and DBT Measurements

[26] To calculate steric height from the XBT and DBT measurements, it was necessary to estimate the vertical salinity profiles, because the XBT and DBT measurements provide only vertical temperature profiles. In the Kuroshio region south of Japan, *Takano et al.* [1981] showed that the temperature–salinity relation differs by region: the coastal cold water region north of the Kuroshio axis, the offshore warm water region south of the Kuroshio axis, and the transitional region in between. Mean temperature–salinity relations were similarly calculated by region, and salinity

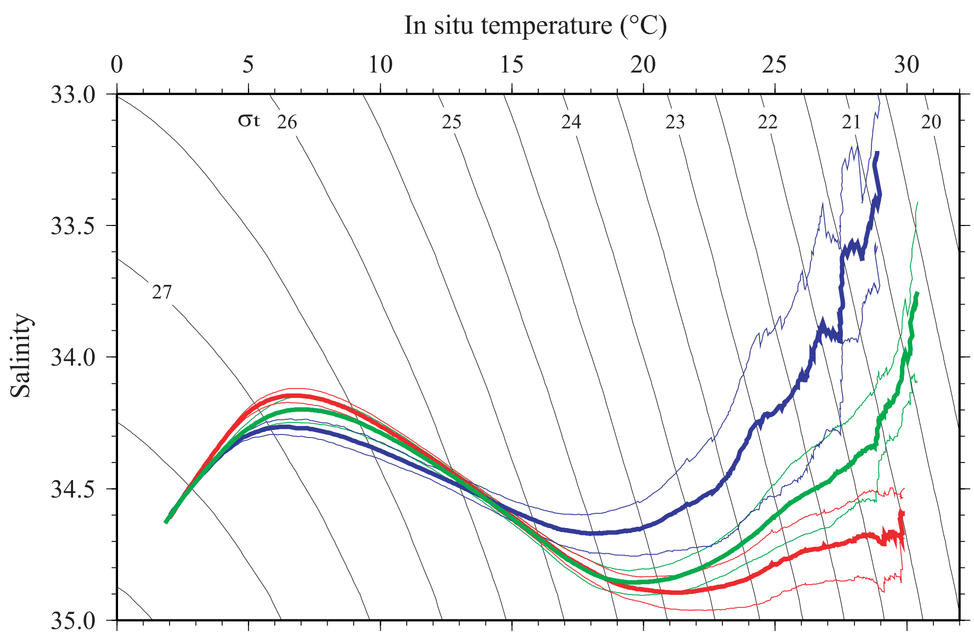

Figure A1. Mean temperature–salinity relationships calculated from CTD data in the coastal cold water region north of the Kuroshio axis (thick blue line), in the region of the stationary local anticyclonic warm eddy south of the Kuroshio axis (thick green line), and in the region south of the warm eddy (thick red line). The thin lines are one standard deviation from the mean of the same color.

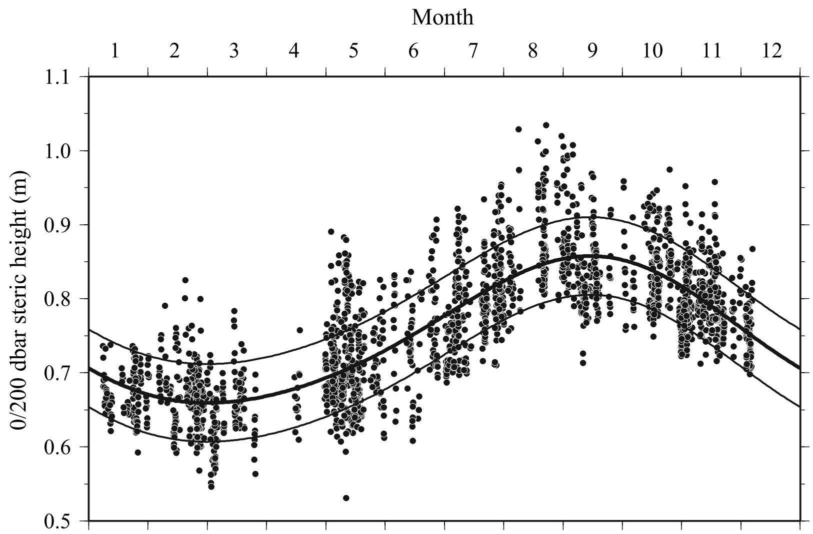

Figure B1. Seasonal cycle of the 0/200 dbar steric height calculated from the ASUKA hydrographic data, without taking account of year or location. The thick line represents the best fitting curve of the sum of annual and semiannual sine curves. The thin lines are one standard deviation (0.052 m) from the fitted curve.

profiles were estimated from the XBT and DBT measurements by using the corresponding mean temperature–salinity relations and XBT and DBT temperature profiles. Along the ASUKA line, the temperature–salinity relation differed by region as follows: (1) the coastal cold water region north of the Kuroshio axis, (2) the region with the local stationary anticyclonic warm eddy [*Hasunuma and Yoshida*, 1978] south of the Kuroshio axis, and (3) the region south of the warm eddy (Figure A1). Transition regions between these were not taken into account. Region 1 was defined as north of 32.3°N or the region where the temperature at 400 dbar was colder than 10.5°C; region 3 was defined as south of 27.8°N; and region 2 was defined as the region between regions 1 and 3. The error (standard deviation) of the 0/700 dbar steric height obtained by using the temperature–salinity relations was estimated to be 0.012 m from 1283 CTD profiles.

Appendix B: Estimation of the 0/700 dbar Steric Height From the Altimeter Data

[27] In section 3, the 0/1800 dbar steric height was estimated from the satellite altimeter data. To compare the steric height calculated from the XBT data with the satellite altimeter data, the 0/700 dbar steric height must be estimated from the altimeter-derived 0/1800 dbar steric height. Along the ASUKA line, the relationships between temperature and salinity were fairly tight (Appendix A), and the temperature profile fluctuated mainly for two reasons: changes in the surface layer due mainly to seasonal changes in the surface heat flux; and heaving of the thermocline, due mainly to the lateral shifting of the Kuroshio axis and passage of cyclonic/anticyclonic eddies across the ASUKA line. Therefore, the 0/700 dbar steric height can be estimated from the 0/1800 dbar steric height as follows. First, the 200/1800 dbar steric height was estimated by subtracting the mean seasonal cycle of the 0/200 dbar steric height (Figure B1) from the 0/1800 dbar steric height. Next, the 200/700 dbar steric height was estimated from the 200/1800 dbar steric height by using the relationship between the 200/1800 dbar steric height and the 200/700 dbar steric height (Figure B2). Finally, the 0/700 dbar steric height was estimated by adding the mean seasonal cycle of the 0/200 dbar steric height to the 200/700 dbar steric height. The error (standard

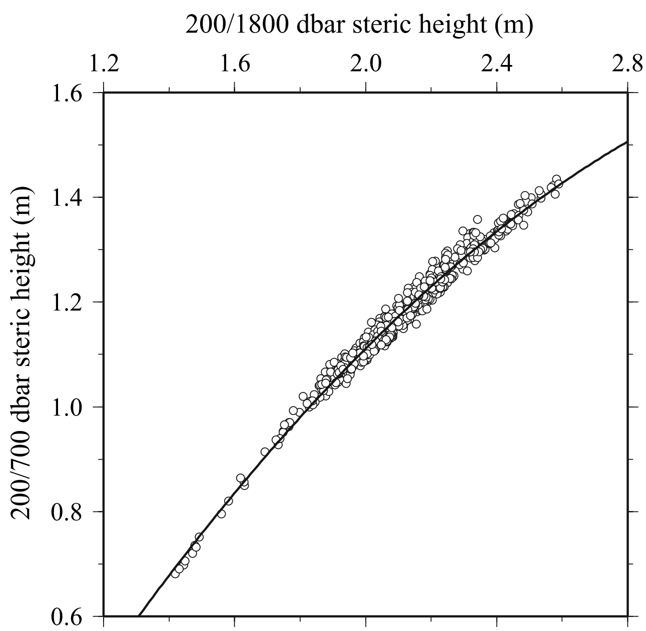

Figure B2. Scatterplot of the 200/700 dbar steric height against the 200/1800 dbar steric height calculated from the ASUKA CTD data. The line represents the best fitting curve of a second-order polynomial. The standard deviation from the fitted curve was 0.015 m.

deviation) in the 0/700 dbar steric height thus obtained was estimated to be 0.029 m from 786 CTD profiles.

[28] **Acknowledgments.** The altimeter products were produced by SSALTO/DUACS and distributed by AVISO with support from the Centre National d'Etudes Spatiales (CNES). The tide gauge data and atmospheric pressure data from the tide gauge station were distributed by the JMA. Most of the ship-based hydrographic data along the ASUKA line were obtained by the ASUKA Group and, especially, the JMA. The hydrographic data from cruise KY04–12 of the R/V *Kaiyo* were obtained by the Kuroshio Transport and Surface Flux Group of IORGC/JAMSTEC. The hydrographic data from cruise 318M200406 (WHP P2 reoccupation) of the R/V *Melville* were distributed by the CLIVAR and Carbon Hydrographic Data Office. Argo data were collected and made freely available by the International Argo Project and the national initiatives that contribute to it (http://www.argo.ucsd.edu, http://argo.jcommops.org). Argo is a pilot program of the Global Ocean Observing System. The PIES observations were jointly carried out with Mark Wimbush (University of Rhode Island) and Hirohiko Nakamura (Kagoshima University). We thank Hiroyuki Nakajima (Marine Works Japan, Ltd.) for finding large salinity biases in a part of the Argo float data. Comments by Kaoru Ichikawa (Kyushu University) and two anonymous reviewers helped to improve the paper. A part of this study was supported by a Grant-in-Aid for Scientific Research (B) (18340142) from Japan Society for the Promotion of Science, Japan.

References

de Boor, C. (2001), *A Practical Guide to Splines*, rev. ed., 346 pp. Springer, New York.

Gouretski, V., and K. P. Koltermann (2007), How much is the ocean really warming?, *Geophys. Res. Lett.*, *34*, L01610, doi:10.1029/2006GL027834.

Hanawa, K., and H. Mitsudera (1985), On the data processing of daily mean values of oceanographic data: Note on the daily mean sea-level data (in Japanese), *Bull. Coastal Oceanogr.*, *23*, 79–87.

Hanawa, K., P. Rual, R. Bailey, A. Sy, and N. Szabados (1995), A new depth-time equation for Sippican or TSK T-7, T-6 and T-4 expendable bathythermograph (XBT), *Deep Sea Res.*, *42*(8), 1423–1451, doi:10.1016/0967-0637(95)97154-Z.

Hasunuma, K., and K. Yoshida (1978), Splitting of the subtropical gyre in the western North Pacific, *J. Oceanogr.*, *34*, 160–172.

Imawaki, S., H. Uchida, H. Ichikawa, M. Fukasawa, S. Umatani, and ASUKA Group (2001), Satellite altimeter monitoring the Kuroshio transport south of Japan, *Geophys. Res. Lett.*, *28*, 17–20, doi:10.1029/2000GL011796.

Isobe, A., and S. Imawaki (2002), Annual variation of the Kuroshio transport in a two-layer numerical model with a ridge, *J. Phys. Oceanogr.*, *32*, 994–1009, doi:10.1175/1520-0485(2002)032<0994:AVOTKT>2.0.CO;2.

Isobe, A., M. Kamachi, Y. Masumoto, H. Uchida, and T. Kuragano (2004), Seasonality of the Kuroshio transport revealed in a Kuroshio assimilation system, *J. Oceanogr.*, *60*, 321–328, doi:10.1023/B:JOCE.0000038338.05850.5e.

Kakinoki, K., S. Imawaki, H. Uchida, H. Nakamura, K. Ichikawa, S. Umatani, A. Nishina, H. Ichikawa, and M. Wimbush (2008), Variations of Kuroshio geostrophic transport south of Japan estimated from long-term IES observations, *J. Oceanogr.*, *64*, 373–384, doi:10.1007/s10872-008-0030-4.

Kitagawa, G., and W. Gersch (1996), *Smoothness Priors Analysis of Time Series, Lecture Notes in Statistics*, 116 pp. Springer, New York.

Kizu, S., H. Yoritaka, and K. Hanawa (2005), A new fall-rate equation for T-5 expendable bathythermograph (XBT) by TSK, *J. Oceanogr.*, *61*, 115–121, doi:10.1007/s10872-005-0024-4.

Lemke, P., et al. (2007), Observations: Changes in snow, ice and frozen ground, in *Climate Change 2007: The Physical Science Basis, Contribution of Working Group I to the Fourth Assessment Report of the Intergovernmental Panel on Climate Change*, edited by S. Solomon et al., pp. 337–383, Cambridge Univ. Press, Cambridge, U.K.

Lombard, A., D. Garcia, G. Ramillien, A. Cazenave, R. Biancale, J. M. Lemoine, F. Flechtner, R. Schmidt, and M. Ishii (2007), Estimation of steric sea level variations from combined GRACE and Jason-1 data, *Earth Planet. Sci. Lett.*, *254*, 194–202, doi:10.1016/j.epsl.2006.11.035.

Lyman, J. M., J. K. Willis, and G. C. Johnson (2006), Recent cooling of the upper ocean, *Geophys. Res. Lett.*, *33*, L18604, doi:10.1029/2006GL027033. (Correction to "Recent cooling of the upper ocean", Geophys. Res. Lett., 34, L16601, doi:10.1029/2007GL030323, 2007.)

Munk, W. (2003), Ocean freshening, sea level rising, *Science*, *300*, 2041–2043, doi:10.1126/science.1085534.

Saunders, P. M., and N. P. Fofonoff (1976), Conversion of pressure to depth in the ocean, *Deep Sea Res.*, *23*, 109–111.

Takano, I., S. Imawaki, and H. Kunishi (1981), TS dynamic height calculation in the Kuroshio region, *Mer*, *19*, 75–84.

Teague, W. J., Z. R. Hallock, G. A. Jacobs, and J. L. Mitchell (1995), Kuroshio sea surface height fluctuations observed simultaneously with inverted echo sounders and TOPEX/POSEIDON, *J. Geophys. Res.*, *100*(C12), 24,987–24,994, doi:10.1029/95JC01526.

Uchida, H., S. Imawaki, and J.-H. Hu (1998), Comparison of Kuroshio surface velocities derived from satellite altimeter and drifting buoy data, *J. Oceanogr.*, *54*, 115–122, doi:10.1007/BF02744385.

Uchida, H., T. Kawano, and M. Fukasawa (2008), In situ calibration of moored CTDs used for monitoring abyssal water, *J. Atmos. Oceanic Technol.*, *25*, 1695–1702, doi:10.1175/2008JTECH0581.1.

Watts, D. R., and H. Kontoyiannis (1990), Deep-ocean bottom pressure measurement: Drift removal and performance, *J. Atmos. Oceanic Technol.*, *7*, 296–306, doi:10.1175/1520-0426(1990)007<0296:DOBPMD>2.0.CO;2.

S. Imawaki, Japan Agency for Marine-Earth Science and Technology, Yokosuka, Kanagawa 237-0061, Japan.

H. Uchida, Institute of Observational Research for Global Change, Japan Agency for Marine-Earth Science and Technology, 2-15 Natsushima, Yokosuka, Kanagawa 237-0061, Japan. (huchida@jamstec.go.jp)